Marine Pollution Bulletin 187 (2023) 114579

Contents lists available at ScienceDirect

Marine Pollution Bulletin

journal homepage: www.elsevier.com/locate/marpolbul

The effects of seawater thermodynamic parameters on the oxygen minimum zone (OMZ) in the tropical western Pacific Ocean

Jun Ma [a,b,c,d], Xuegang Li [a,b,c,d,*], Jinming Song [a,b,c,d,*], Lilian Wen [a,b,c,d], Qidong Wang [a,b,c,d], Kuidong Xu [a,b,c,d], Jiajia Dai [a,b,c,d], Guorong Zhong [a,b,c,d]

[a] CAS Key Laboratory of Marine Ecology and Environmental Sciences, Institute of Oceanology, Chinese Academy of Sciences, Qingdao 266071, China
[b] Laboratory for Marine Ecology and Environmental Science, Pilot National Laboratory for Marine Science and Technology (Qingdao), Qingdao 266237, China
[c] University of Chinese Academy of Sciences, Beijing 100049, China
[d] Center for Ocean Mega-Science, Chinese Academy of Sciences, Qingdao 266071, China

ARTICLE INFO

Keywords:
Oxygen minimum zone
Tropical western Pacific Ocean
Temperature
Salinity
Density

ABSTRACT

The continuous expansion of the oxygen minimum zone (OMZ) is a microcosm of marine hypoxia problem. Based on a survey in M4 seamount area of Tropical Western Pacific Ocean, the effects of thermodynamic parameters on OMZ were discussed. The study showed thermodynamic parameters mainly affect the upper oxycline of OMZ. The increase in temperature aggravates seawater stratification, which not only shallows oxycline but also increases the strength of DO stratification, promoting the expansion of OMZ. Based on relationships between thermodynamic parameters, water mass and DO, OMZ in this area is defined as follows: the water layer with low DO between the lower boundary of high-salt area and 1000 m. Moreover, the study showed that though there is no "seamount effect" on a scale of 3000 m, low-value areas of DO form at the bottom of seamount. This study will provide an evidence for expansion of OMZ exacerbated by global warming.

1. Introduction

Marine hypoxia is growing increasingly severe as a result of global warming, generating a slew of ecological issues (Schmidtko et al., 2017; Bertagnolli and Stewart, 2018). The oxygen minimum zone (OMZ) is a water layer in the ocean with dissolved oxygen (DO) levels below a certain threshold, indicating a low oxygen environment (Stramma et al., 2008; Paulmier and Ruiz-Pino, 2009; Keeling et al., 2010; Ma et al., 2021d; Wang et al., 2021). The rapid expansion of OMZs reflects the global marine hypoxia problem, and its extent has increased dramatically on both vertical and horizontal scales in the Pacific, Indian, and Atlantic Oceans during the past few decades (Stramma et al., 2008; Stramma et al., 2012; Schmidtko et al., 2017). OMZs are divided into three subzones: the upper oxycline, the OMZ core, and lower oxycline (Paulmier and Ruiz-Pino, 2009; Stramma et al., 2012). Surprisingly, the DO concentration in the OMZ core in the eastern Pacific and North Indian Oceans was below the detection limit (Bulow et al., 2010; Ito and Deutsch, 2013; Al Azhar et al., 2017; Saito et al., 2020).

Many studies have investigated the ecological effects of OMZs. The expansion of OMZs transforms the habitats of marine organisms, causing fundamental changes in their distribution patterns and having a considerable effect on marine biodiversity (Stramma et al., 2010; Engel et al., 2022). Meanwhile, OMZs are critical to material cycling, regulating the migration and transformation of various materials, and influencing global carbon and nitrogen cycles (Bulow et al., 2010; Keil et al., 2016; Pachiadaki et al., 2017; Saito et al., 2020). In addition, changes in OMZs are not only a response to climate change, but also stimulate the production of greenhouse gases such as N_2O, thereby accelerating global warming (Naqvi et al., 2010; Shenoy et al., 2020). However, little research on the structure of OMZs has been conducted, particularly in the tropical western Pacific Ocean, which is the primary OMZ formation and growth area. There is a considerable OMZ structure in this region, but relatively high DO concentrations (Paulmier and Ruiz-Pino, 2009; Stramma et al., 2009; Ma et al., 2021d), making it difficult to accurately assess and capture the scope of the OMZ, which will have a large impact on the subsequent assessment of the ecological consequences of the OMZ and the variation law of the OMZ in this region.

Thermodynamic factors such as temperature, salinity, and density

---

[*] Corresponding authors at: CAS Key Laboratory of Marine Ecology and Environmental Sciences, Institute of Oceanology, Chinese Academy of Sciences, Qingdao 266071, China.

E-mail addresses: lixuegang@qdio.ac.cn (X. Li), jmsong@qdio.ac.cn (J. Song).

https://doi.org/10.1016/j.marpolbul.2023.114579
Received 20 November 2022; Received in revised form 30 December 2022; Accepted 1 January 2023

are the basic properties of seawater, and their distributions and variations influence and control the spatiotemporal distribution patterns of other parameters (Yang et al., 2017; Fawcett et al., 2018; Chu and Fan, 2019; Johari and Akhir, 2019; Sánchez-Leal et al., 2020). Vertical diurnal migration of zooplankton occurs in the ocean, and zooplankton always migrate to the water layer below the thermocline at night (Hazen and Johnston, 2010; Lee et al., 2011; Priou et al., 2021). The thermocline and high-salt area hinder the upward transport of nutrients, forming a critical boundary between the upper oligotrophic water level and lower eutrophic water level in the tropical western Pacific Ocean (Williams and Grottoli, 2010; Ma et al., 2020b; Ma et al., 2021a). The thermocline also promotes the dissipation of sound waves in seawater, which is not conducive to sound propagation (Keeling et al., 2010; Worcester et al., 2013; Dzieciuch, 2014). Many studies have indicated that global warming accelerates the deoxygenation process in seawater and is the primary cause of the expansion of the OMZ (Stramma et al., 2008; Schmidtko et al., 2017; Resplandy, 2018). From this perspective, there is a relationship between temperature and DO in seawater, but it is only described qualitatively. In the section of the ocean over kilometers, the relationships between the thermodynamic parameters (temperature, salinity, density, and DO), and how they impact the vertical structure of DO and the properties of OMZs remains unknown.

This study focused on the OMZ in the tropical western Pacific Ocean, using the M4 seamount as an example, to investigate the effects of thermodynamic parameters such as temperature, salinity, and density on the DO structure, as well as the interrelationships between these parameters and the OMZ. This work can serve as a reference for further research on global warming and OMZ in the tropical western Pacific Ocean.

2. Materials and methods

2.1. Study area

The M4 seamount area (140.03–140.36°E, 9.97–10.75°N) (Fig. 1) is located in the tropical western Pacific Ocean, at the core of the western Pacific warm pool (125°-165°E, 0°-16°N) (Gan and Wu, 2012; Zhan et al., 2013), which is a typical oligotrophic, low-productivity sea area in the global ocean (Ma et al., 2019; Ma et al., 2020a; Ma et al., 2023). In May 2019, the *Science* Survey Vessel was used to investigate the M4 seamount area; a total of 25 stations were set up in the form of cross sections above the seamount, which were divided into sections A, B, and C. Sections A and C intersect at station O1 (106 m water depth), and Sections B and C intersect at station O2 (water depth 810 m). Based on the distance between the seamount summit and the water surface, seamounts are classified as shallow (0–200 m), medium-depth (200–400 m), and deep (>400 m) (Genin, 2004; Ma et al., 2021b). According to this classification, the summit on the northern side of the M4 seamount is shallow, whereas the summit on the southern side is deep.

2.2. Data acquisition

During the sampling, the *Science* Survey Vessel used a dynamic positioning system to ensure the position during sampling. Water samples were collected at depths of 0, 30, 50, 75, 100, 150, 200, 300, 500, 1000, 2000, and 3000 m using a Niskin water collector (KC-Denmark, Denmark). Temperature, salinity, density, and DO were among the parameters measured.

A conductivity-temperature-depth (CTD) instrument (Sea-bird SBE911, USA) was used to simultaneously measure temperature, salinity, and density when water samples were collected. The CTD was rigorously calibrated before use, and the accuracies of temperature, salinity, and density readings were 0.001 Â °C, 0.0003 S/m, and 0.0001 kg/m^3, respectively.

DO was initially determined using the Winkler iodometric method. Water from each layer (50 mL) was collected in a brown bottle. After fixing by adding manganese chloride and an alkaline potassium iodide solution, the water was titrated with sodium thiosulfate to calculate the DO concentration, with a standard deviation (SD) of <0.02 (Ma et al., 2020a; Ma et al., 2021d; Wen et al., 2022). The DO sensor on the CTD was then used to measure DO when the water samples were collected, and the DO at full water depth was compared and corrected using the DO measured by the iodometric method.

To compare the sampling stations, we obtained 1° × 1° data for temperature, salinity, and DO from the World Ocean Atlas 2018 (Ma et al., 2021d).

3. Results

3.1. Hydrological characteristics of the M4 seamount area

According to the T-S diagram (Fig. 2) and related reports (Gan and Wu, 2012; Hu et al., 2015; Ma et al., 2020a), the water mass in this region can be divided into Surface Water (SW), North Pacific Tropical Water (NPTW), North Pacific Intermediate Water (NPIW), and deep water (DW). SW is located at 0–30 m and is characterized by high

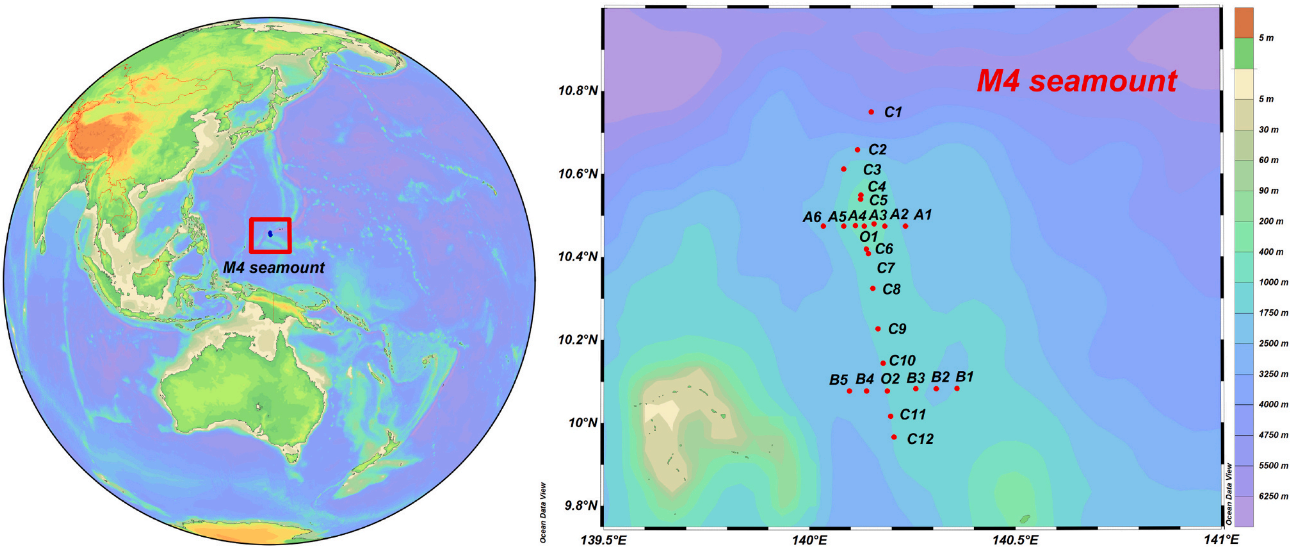

Fig. 1. Map of the M4 seamount area.

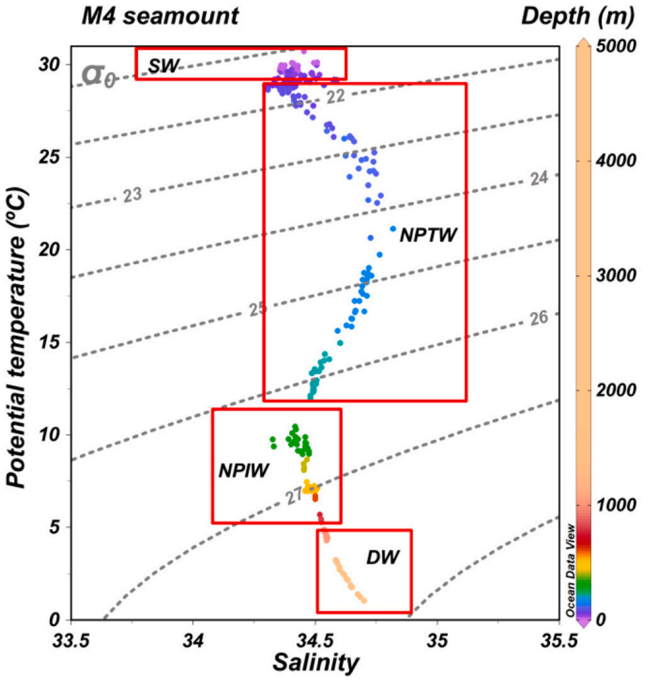

Fig. 2. Characteristics of water mass in the M4 seamount area.
SW: Surface Water; NPTW: North Pacific Tropical Water; NPIW: North Pacific Intermediate Water; DW: Deep Water.

temperature and low salinity (average temperature is 29.68 °C; average salinity is 34.41). NPTW is located at 50–200 m and is characterized by high salinity and large temperature change (average salinity is 34.54; temperature range is 11.96–29.62 °C). NPIW is located at 300–800 m and is characterized by reduced temperature and stable salinity (temperature range is 5.36–10.49 °C; average salinity is 34.46). DW is located at depths >1000 m and is characterized by low temperature and high salinity (average temperature is 3.56 °C; average salinity is 34.59) (Table 1).

Temperature, salinity, and density exhibited similar vertical distributions at each station (Fig. 3a,b,c). These parameters remain constant in the upper water levels (0–30 m), where there are strong thermoclines, high-salt areas, and pycnoclines, and fluctuate slowly and remain stable as water depth increases. Using the vertical gradient method (0.05 °C/m) and the inflection point method to determine the range of the thermocline (Zhang et al., 2006; Fiedler, 2010; Chu and Fan, 2019), the upper boundary of the thermocline (UT) was 81 m, the lower boundary of the thermocline (LT) was 203 m, and the temperature gradient was determined was 13.15 °C/hm (Fig. 3d). Under the influence of NPTW with high salinity, there were evident high-salt areas in the vicinity of the M4 seamount. Using the inflection point method to determine the range of the high-salt area (Wang et al., 2013; Ma et al., 2020b), the upper boundary of the high-salt area (US) was 46 m, its lower boundary (LS) was 265 m, and the highest value of salinity (HS) (34.83) in the high-salt area is located at 126 m (Fig. 3e). Using the vertical gradient method (0.015 kg/m^3) and the inflection point method to determine the range of the densitocline (Zhang et al., 2006; Fiedler, 2010; Chu and Fan, 2019), the upper boundary of the pycnocline (UP) was 77 m, its lower boundary (LP) was 173 m, and the density gradient was 4.73 (kg/m^3)/hm (Fig. 3f).

Fig. 4 shows the positional relationship of the thermocline, high-salt area, and pycnocline. The thermocline and the pycnocline practically coincide, and the HS in the high-salt area is in the center of the thermocline and the pycnocline. The thermocline and pycnocline are enclosed by the high-salt area, which has the largest range. The density of seawater is a function of temperature, salinity, and depth (Safarov et al., 2009; Pawlowicz et al., 2012), and temperature and salinity have a direct effect on seawater density with little change in depth. In this study, the salinity at 46–265 m is high due to the presence of a high-salt area, and the density is directly controlled by temperature at this time; therefore, the boundaries of the thermocline and pycnocline are essentially the same. As water depth increases, so does density, which increases with decreasing temperature and increasing salinity.

3.2. *Analysis of DO structure in the M4 seamount area*

The DO at each station had similar vertical distributions. The DO concentration is high in the upper water levels, and then drops sharply as water depth increases, forming an upper oxycline in which DO is at a minimum. After that, DO remains low before gradually rising to form the lower oxycline as water depth increases (Fig. 5a). The upper oxycline ranged from 89 m with a DO concentration of 6.55 mg/L to 330 m with a DO concentration of 2.92 mg/L; its gradient was 1.53 (mg/L)/hm. The DO concentration remained low at 330–1111 m, increasing slightly to 3.56 mg/L at 548 m. It also increased slowly at water depths >1111 m, forming a lower oxycline (Fig. 5b). Note that OMZ refers to the water layer with DO concentrations lower than a certain threshold and a considerable DO oxycline between it and the upper and lower water levels (Paulmier and Ruiz-Pino, 2009; D'Asaro et al., 2020; Ma et al., 2021d). We found considerable DO oxyclines in the upper and lower water levels, as well as a minimum DO value, confirming the presence of the OMZ structure in the M4 seamount area. However, using the conventional thresholds of 100 μmol/L (3.20 mg/L), 90 μmol/L (2.88 mg/L) or 60 μmol/L (1.92 mg/L) to divide the OMZ range (Karstensen et al., 2008; Stramma et al., 2008; Paulmier and Ruiz-Pino, 2009; Levin, 2018), there is only a small or no OMZ distribution in the water column in the M4 seamount area, which is clearly inaccurate. The findings of this study also show that the OMZ range cannot be simply divided using the threshold method for the Tropical Western Pacific Ocean and other sea areas with generally high DO concentrations, resulting in a considerable systematic deviation.

4. Discussion

4.1. *Effects of the M4 seamount on DO*

Seamounts are common landforms in deep oceans, referring to uplifts that protrude >1000 m above the seafloor (Yesson et al., 2011; Ma et al., 2021b; Xu, 2021). Affected by the unique topography, the hydrological environment around seamounts is complex and often induces

Table 1
T, salinity and DO of water masses in the M4 seamount area.

Water mass	Depth (m)	T (°C)		Salinity		DO (mg/L)	
		Range	Average	Range	Average	Range	Average
SW	0–30	29.07–30.71	29.68	34.33–34.52	34.41	6.34–6.65	6.47
NPTW	50–250	11.96–29.62	22.70	34.29–34.82	34.54	4.00–6.69	5.78
NPIW	300–800	5.36–10.49	8.16	34.33–34.53	34.46	2.92–3.51	3.25
DW	≥1000	1.48–4.95	3.56	34.54–34.70	34.59	3.02–5.72	3.55

Note: SW: Surface Water; NPTW: North Pacific Tropical Water; NPIW: North Pacific Intermediate Water; DW: Deep Water.

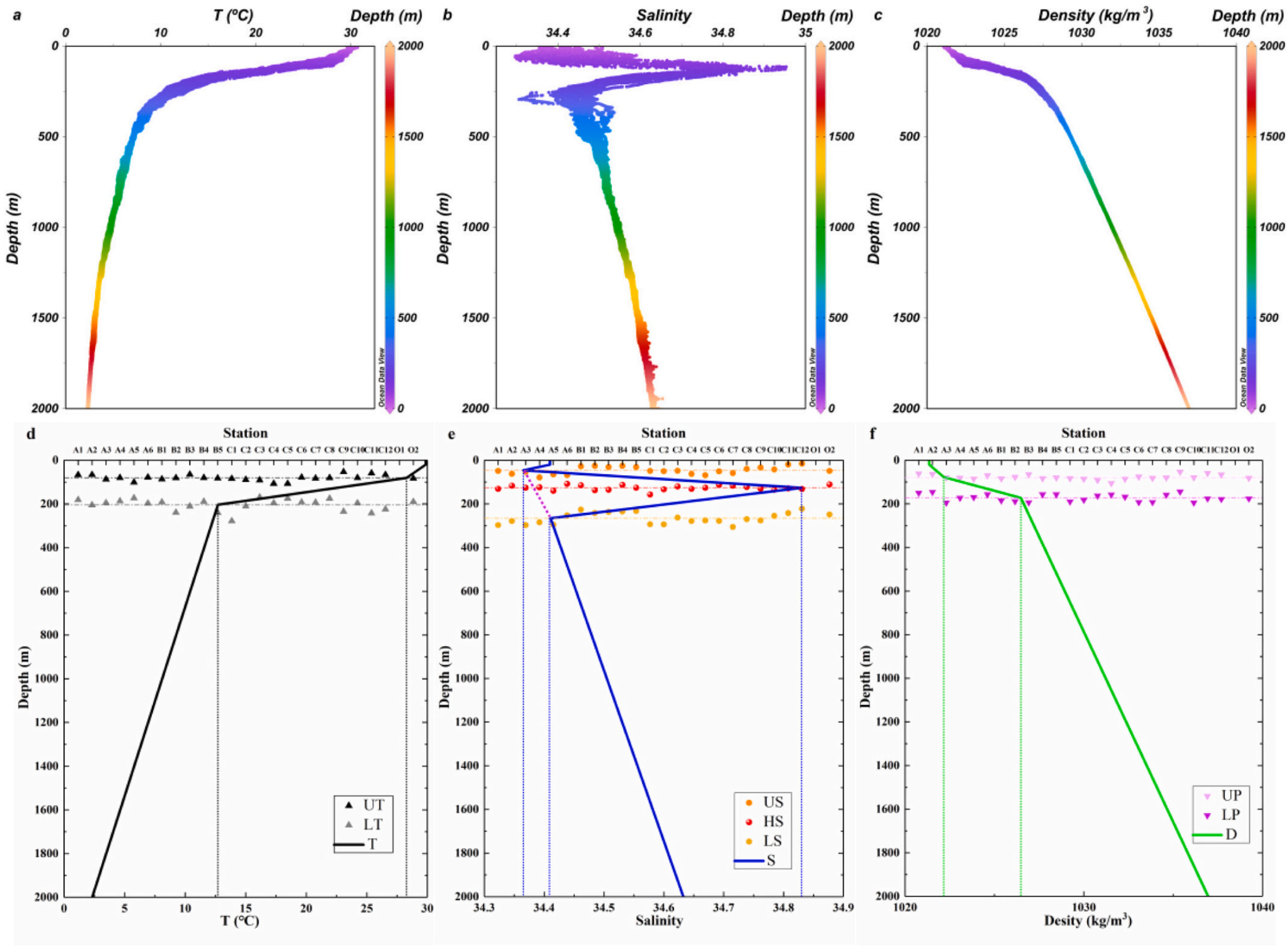

Fig. 3. Vertical distribution of T, salinity and density in the M4 seamount area.
UT: Upper boundary of thermocline; LT: Lower boundary of thermocline; US: Upper boundary of high-salt area; HS: Highest value of salinity; LS: Lower boundary of high-salt area; UP: Upper boundary of pycnocline; LP: Lower boundary of pycnocline.

relatively isolated ecosystems, which causes the distribution of substances and the composition of biological communities to differ substantially from those in other regions (Genin, 2004; Clark et al., 2010). Upwelling often occurs around seamounts, promoting the upward transport of high nutrient concentrations from the bottom into the euphotic layer (<200 m), which is conducive to plankton growth and reproduction, as well as the accumulation of other organisms, culminating in the "seamount effect" (Misic et al., 2012; Dai et al., 2020). Because upwelling is difficult to observe directly, the uplift of the isotherm is the main reference for upwelling (Ana et al., 2012; Ma et al., 2020a; Ma et al., 2020b). The isotherm in the M4 seamount area exhibited no evident relationship with the position of the seamount on a scale of 3000 m (Fig. 6a,b,c), indicating that the seamount may not generate upwelling. Similarly, there was also no evident relationship between the distribution of DO and the location of the M4 seamount (Fig. 6d, e, f). Here, the M4 seamount acts as a simple physical barrier that directly blocks the distribution of DO. This result also suggests that there may be no upwelling around the M4 seamount at a scale of 3000 m.

The hydrological environment around the seamount is complex, and not all seamounts can induce upwelling. Even for the same seamount, it is not always possible to detect upwelling in each observation. For example, among the three surveys conducted in the Minami-kasuga seamount in the tropical western Pacific Ocean, Genin and Boehlert (1985) found a cold dome caused by upwelling observed in the first survey, although upwelling was recorded in both the second and third surveys. MouriÑO et al. (2001) conducted five surveys on the Great Meteor seamount in the subtropical northeastern Atlantic Ocean, and they found that seasonal factors have a considerable influence on upwelling. In the first survey, an isotherm of 19.3 °C was found to rise from 150 m to sea level, indicating the occurrence of upwelling, whereas no substantial upwelling was found in other surveys. Ma et al. (2021c) found an upwelling in the M4 seamount area, as well as the circulation in their investigation in August 2017, that is, there is a Taylor column around the M4 seamount area, and the presence of the Taylor column makes the obvious increase of nutrients, Chlorophyll a and heterotrophic bacteria around the summit of the seamount to form a "seamount effect". The second survey in May 2019 was conducted in the M4 seamount area. Not only did we not find Taylor columns, but also did not find an upwelling around the M4 seamount area, indicating complexity of the hydrological environment around the seamount, and that the survey can only show the results of this time.

Although no seamount effect was observed around the M4 seamount on a scale of 3000 m in this survey, the presence of the M4 seamount still has a certain impact on the DO distribution. At 1250 m in section A and at 500 and 1000 m in section C, the DO concentration (<3 mg/L) at stations near the seamount was considerably lower than that at stations far from the seamount. The topography of the seamount is not only conducive to the formation of an upwelling but also to the accumulation and retention of organic matter, making it an ideal habitat for benthic

)

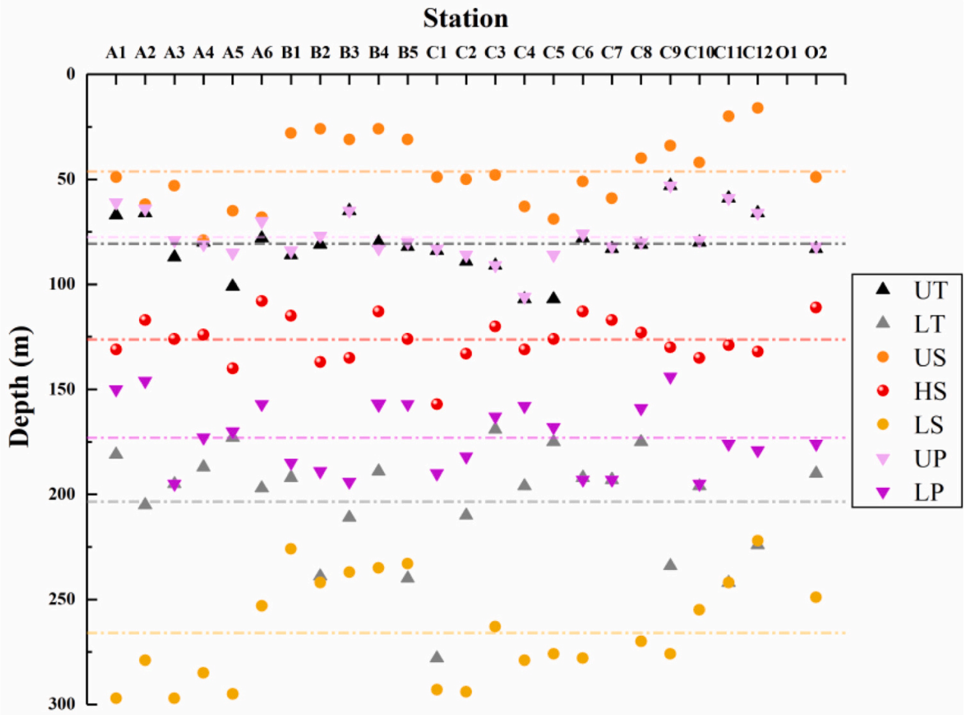

Fig. 4. Water depth of thermocline, high-salt area and pycnocline in the M4 seamount area.
UT: Upper boundary of thermocline; LT: Lower boundary of thermocline; US: Upper boundary of high-salt area; HS: Highest value of salinity; LS: Lower boundary of high-salt area; UP: Upper boundary of pycnocline; LP: Lower boundary of pycnocline.

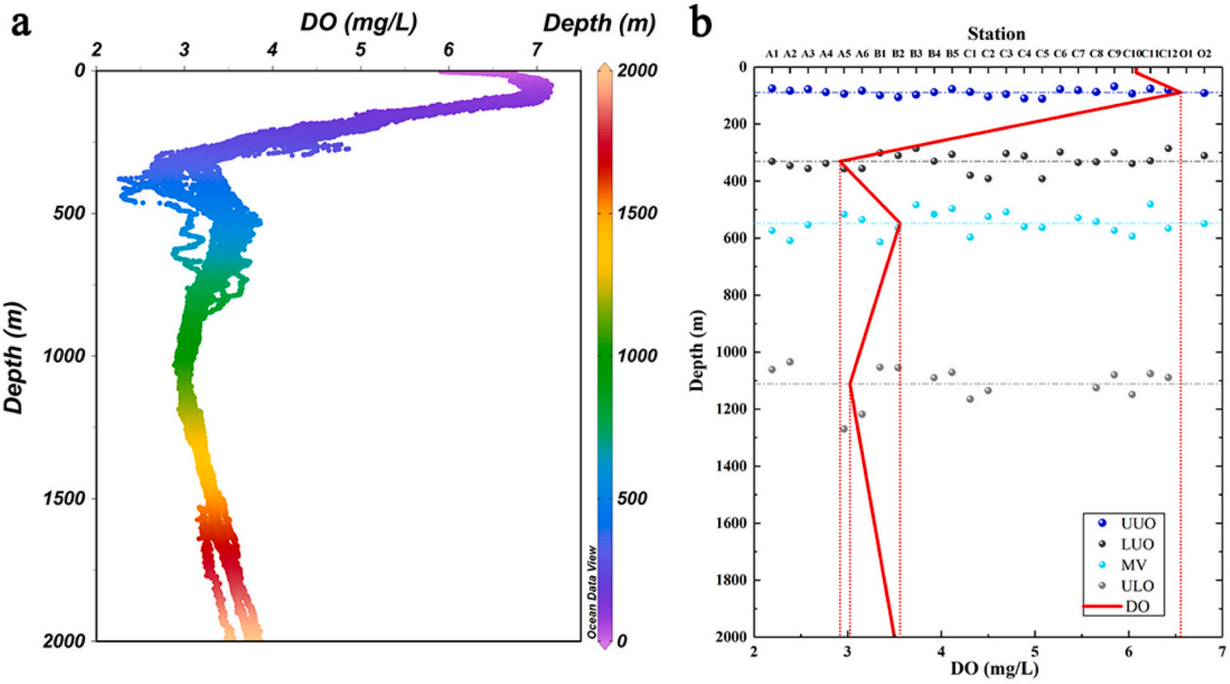

Fig. 5. DO structure in the M4 seamount area. a) Vertical distribution of DO, b) Relative location of different boundaries.
UUO: Upper boundary of upper oxycline; LUO: Lower boundary of upper oxycline; MV: Maximal value of DO; ULO: Upper boundary of lower oxycline.

organisms (Morgan et al., 2019; Shen et al., 2021; Bridges et al., 2022; Lai et al., 2022).

Duineveld et al. (2004) found a coral forest at about 800 m on the Galicia seamount in the northwestern Spanish Sea, and benthic organisms near the coral forest contributed greatly to the decomposition of organic matter in this area. Xu et al. (2021) also found large coral forests on multiple seamounts in the tropical western Pacific Ocean, which were surrounded by a plethora of benthic organisms and organic debris. In particular, large coral forests as well as several new benthic species were discovered during surveys of the M4 seamount in 2017 and 2019, demonstrating the presence of abundant benthic organisms and organic matter in the M4 seamount region (Li et al., 2021; Wu et al., 2021; Xu

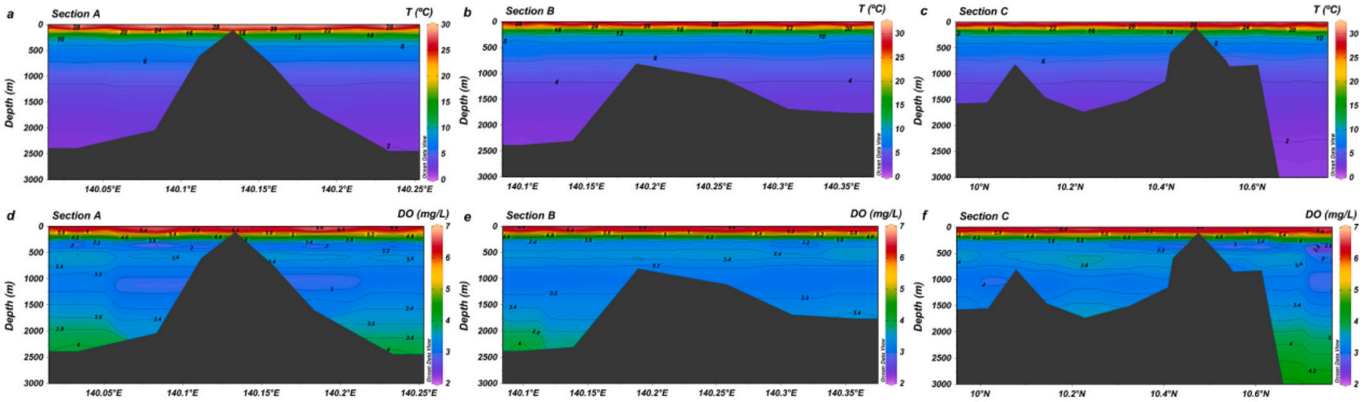

Fig. 6. Vertical distribution of T and DO in section A,B and C of the M4 seamount area. a) T in section A, b) T in section B, c) T in section C, d) DO in section A, e) DO in section B, f) DO in section C.

et al., 2021). The activities of benthic organisms and decomposition of organic matter consume a large quantity of DO, resulting in a dramatic drop in DO in a certain area. In this study, the DO concentration decreased considerably at stations near the M4 seamount, which may be related to the abundance of benthic organisms and organic matter in this area.

4.2. *Influence of thermodynamic parameters on the structure of OMZ*

For a more intuitive comparison, stations A1, B1, and C1 from the three sections were selected to explore the relationship between DO, temperature, salinity, and density. As shown in Fig. 7, the thermocline ranges at the three stations are 67–181 m, 86–192 m, and 84–278 m, respectively, whereas the upper oxycline ranges are 75–331 m, 99–301 m, and 87–380 m, respectively. The upper and lower oxycline boundaries at each station are slightly deeper than the upper and lower thermocline boundaries (Fig. 7a,b,c). The ranges of the high-salt areas at A1, B1, and C1 were 49–297 m, 28–226 m, and 49–293 m, respectively, whereas the lower boundaries of the upper oxycline (LUO) or depths of minimum DO concentration were 331 m, 301 m, and 380 m, respectively, just below the high-salt area (Fig. 7d,e,f). The pycnoclines at A1, B1, and C1 ranged from to 61–150 m, 84–185 m, and 83–190 m, respectively, and were shallower and narrower than the upper oxyclines (Fig. 7g,h,i). In this study, the high-salt area had a wider range than the thermocline and the pycnocline, and density was directly controlled by temperature under conditions of low depth change and salinity, resulting in essentially consistent thermocline and pycnocline boundaries. This phenomenon has been reported in at several locations around the tropical western Pacific Ocean (Wang et al., 2000; Wang et al., 2013; Ma et al., 2020b). Furthermore, the DO at each station in the M4 seamount area was closely related to temperature, salinity, and density (Fig. 7j), which was primarily manifested in the control of the upper oxycline by the cline of thermodynamic parameters and high-salt areas; that is, the upper boundary of the upper oxycline (UUO) was located below the UT and the UP, and the LUO was located below the lower boundary of the high-salt area (LS).

The above results indicate that each thermodynamic parameter has a certain relationship with the boundary of the DO structure in the vertical position. However, the exact mechanism by which these thermodynamic parameters affect DO structure is unknown. In this study, the UT and UP were positively correlated with the UUO ($r = 0.72$, $r = 0.69$, $P < 0.01$; Fig. 8a,b), indicating that the depth at which the thermocline and pycnocline began can directly control the water depth at which the upper oxycline began. This phenomenon has been reported in several studies, including a study of the Arabian Sea by Wishner et al. (2008), who also noted that UT and UUO coincide, and that the depth of UT directly impacts the depth of UUO. They also discovered that the depth at which the sharp changes in temperature and DO begin is similar in the eastern tropical North Pacific Ocean (Wishner et al., 2013). In recent years, the influence of global warming on marine deoxygenation, which exacerbates seawater stratification and further inhibits seawater ventilation, has received considerable attention (Stramma et al., 2008; Schmidtko et al., 2017; Li et al., 2020). In this study, the thickness of the thermocline (TT) was significantly negatively correlated with UUO ($r = -0.31$, $P < 0.01$) (Fig. 8c), indicating that the stronger the thermocline, the shallower the upper oxycline; hence, stronger seawater stratification exacerbates DO stratification. Moreover, the gradient of the thermocline (GT) was closely related to the gradient of the pycnocline (GP) (Fig. 8j), which had a direct effect on the gradient of the upper oxycline (GUO) ($r = 0.64$, $r = 0.58$, $P < 0.01$) (Fig. 8k,l), implying that increased seawater stratification exacerbates DO stratification, thereby increasing the strength of the OMZ. This conclusion could explain the influence of global warming on the expansion of the OMZ; that is, an increase in temperature aggravates seawater stratification, which not only makes the oxycline shallower but also increases the intensity of the DO stratification, thereby promoting the expansion of the OMZ. The LUO was closely related to the US and LS ($r = 0.56$, $r = 0.59$, respectively; $P < 0.01$) but was not with the thermocline (Fig. 8d,e,f), indicating that the LUO may be primarily controlled by the high-salt area. The high-salt area in the tropical western Pacific Ocean is controlled by NPTW, which is characterized by significant interannual and seasonal variability (Wang et al., 2013; Ma et al., 2020b). The close relationship between LUO and the high-salt area may indicate that LUO also exhibits interannual and seasonal variations. DW was at depths >1000 m in the tropical western Pacific Ocean, and the DO in the DW was considerably higher than that in the NPTW (Table 1). The DW is primarily controlled by Antarctic Intermediate Water (AAIW) and Antarctic Bottom Water (AABW), which are characterized by low temperature, high salinity, and low oxygen (Holzer and Primeau, 2006; Kawabe and Fujio, 2010). In this study, the ULO was not significantly correlated with temperature, density, or salinity (Fig. 8g, j, i), indicating that thermodynamic factors may not have an effect on the lower oxycline, and that water mass may have a major impact on the ULO.

Based on the above analysis, it is clear that the UUO is controlled by the thermocline and pycnocline, the LUO by the high-salt area, and the ULO by water masses such as AAIW and AABW. Fortunately, the OMZ structure can be described more clearly with these DO structure boundaries. As previously noted, merely defining the OMZ range using the DO threshold may be inapplicable to the study of the OMZ in the tropical western Pacific Ocean. There are remarkable DO oxyclines between the OMZ and the upper and lower water levels (Paulmier and Ruiz-Pino, 2009; D'Asaro et al., 2020; Ma et al., 2021d), Based on the relationship between thermodynamic parameters and DO (Fig. 7j), we may define the OMZ in the tropical western Pacific Ocean as follows: a

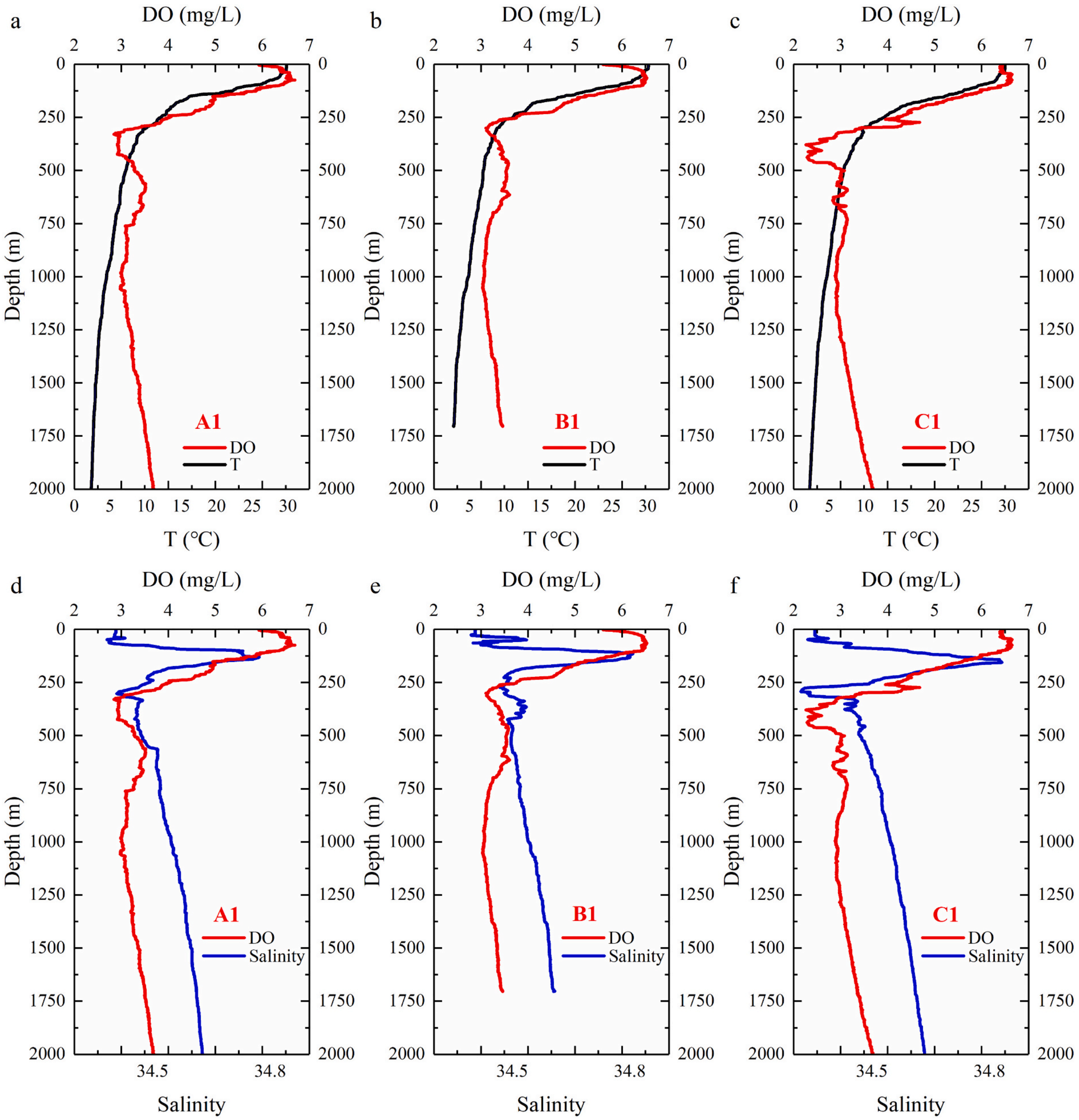

Fig. 7. Vertical distribution relationship of DO with T, salinity and density in the M4 seamount area.
UT: Upper boundary of thermocline; LT: Lower boundary of thermocline; US: Upper boundary of high-salt area; HS: Highest value of salinity; LS: Lower boundary of high-salt area; UP: Upper boundary of pycnocline; LP: Lower boundary of pycnocline; UUO: Upper boundary of upper oxycline; LUO: Lower boundary of upper oxycline; MV: Maximal value of DO; ULO: Upper boundary of lower oxycline.

water layer with low DO concentration between the LS and the 1000 m water layer, with large DO oxyclines between it and the upper and lower water levels. This definition blurs the threshold constraints on the definition of OMZ, highlights the core of the DO structure, and emphasized the influence of thermodynamic factors and water mass characteristics on OMZ. According to this definition, the OMZ at each station in the M4 seamount area (A1, B1, and C1) is located between 266 m and 1000 m, which is more consistent with the basic concept of the OMZ than the threshold method (3.20 mg/L, 310–430 m and 940–1420 m, respectively). In a study of the eastern tropical North Pacific Ocean, Wishner et al. (2013) found that the threshold method cannot be used to easily narrow the range of an OMZ. They used the distribution of plankton to evaluate the OMZ structure and classified it as upper oxycline, OMZ core, and lower oxycline. Paulmier and Ruiz-Pino (2009) also reported that when determining the presence of an OMZ, one should focus on the upper oxycline when summarizing the structural division of the OMZ in the global ocean and finally determine the range of the OMZ in combination with biogeochemical processes. Unfortunately, there has been little discussion of the thermodynamic parameters and structure of OMZs, and there have been no research reports on OMZs in the tropical western Pacific Ocean. Thus, we could not identify relevant studies for comparison.

To validate the findings of this study, we explored the relationship between the OMZ and temperature and salinity across a wider range centered on the M4 seamount in the tropical western Pacific Ocean (Fig. 9a). The vertical distributions of temperature, salinity, and DO at eight stations were virtually identical, and they were also similar to those in the M4 seamount area, indicating that the water mass in the

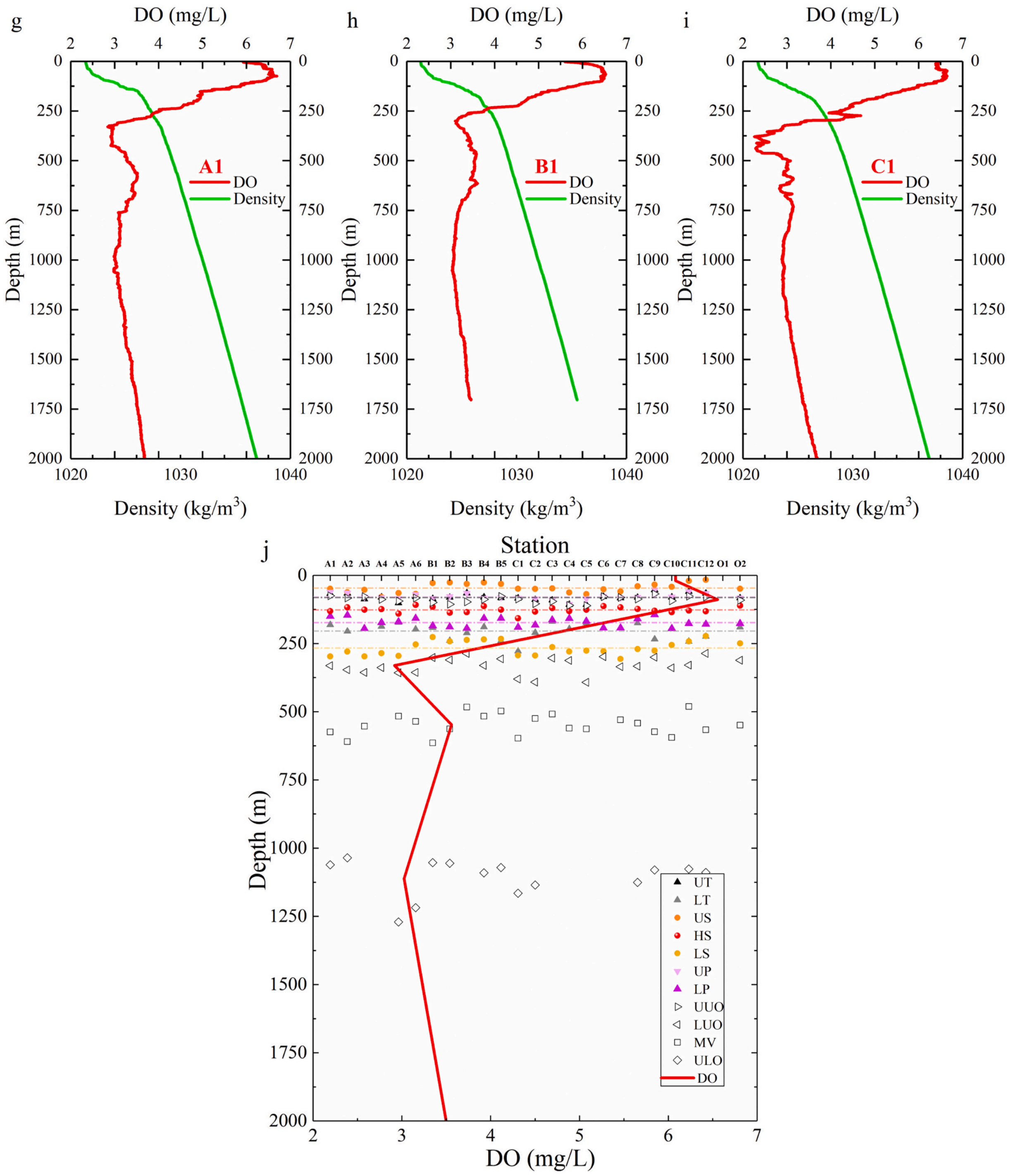

Fig. 7. (*continued*).

tropical western Pacific Ocean is the same, increasing the SW, NPTW, NPIW, and DW (Fig. 2, Fig. 9b,c,d). The UT at the eight stations was at 50–125 m, whereas the UUO was at 45–120 m, and they were positively correlated (Table 2). The US and the LS at the eight stations were at 20–45 m and 225–400 m, respectively, whereas the LUO was just below the high-salt area. The above results are similar to those obtained in the M4 seamount area, indicating that the thermodynamic parameters over a wider range centered on the M4 seamount are closely related to the OMZ, that is, the thermocline controls the UUO and the high-salt area controls the LUO, thereby controlling the range of the OMZ. According to our definition of the studied OMZ, the upper boundary of the OMZ was at 225–400 m, and the lower boundary was at 1000 m.

5. Conclusion

In the context of global warming, marine hypoxia is becoming increasingly severe, resulting in a series of ecological problems, and the OMZ in open ocean is a microcosm of the global marine hypoxia problem. This study explored the effects of thermodynamic factors and seamounts on the OMZ in the tropical western Pacific Ocean, providing a fresh perspective for studying the characteristics and changes in the OMZ.

Seawater stratification was visible in the M4 seamount area. The thermocline was at 81–203 m, the pycnocline was at 77–173 m, and the high-salt area was at 46–265 m. There was a typical OMZ structure on

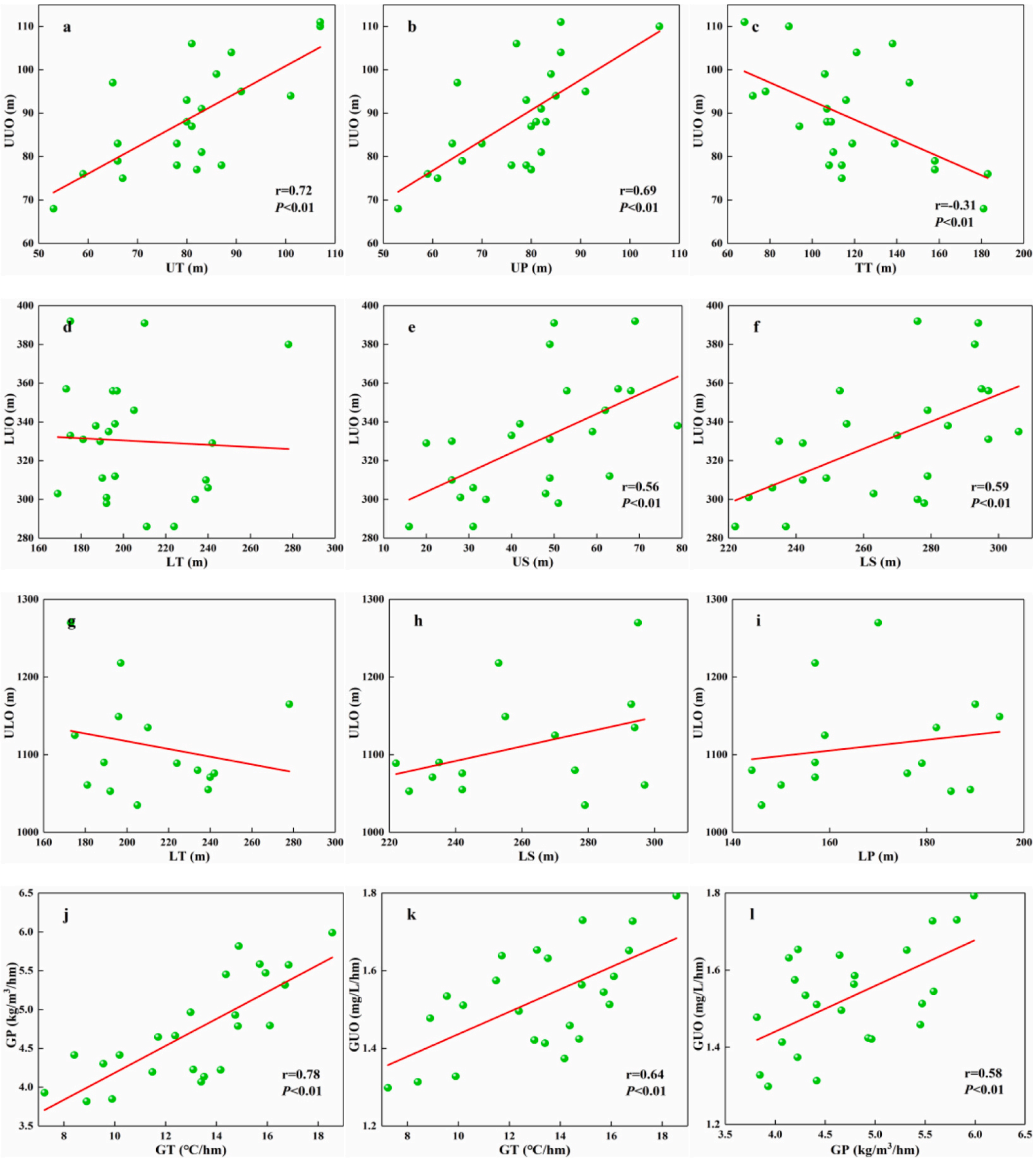

Fig. 8. Correlation analysis of DO with T, salinity and density in the M4 seamount area.
UUO: Upper boundary of upper oxycline; UT: Upper boundary of thermocline; UP: Upper boundary of pycnocline; TT: Thickness of thermocline; LUO: Lower boundary of upper oxycline; LT: Lower boundary of thermocline; US: Upper boundary of high-salt area; LS: Lower boundary of high-salt area; ULO: Upper boundary of lower oxycline; LP: Lower boundary of pycnocline; GP: Gradient of pycnocline; GT: Gradient of thermocline; GUO: Gradient of upper oxycline;

the vertical scale, in which the DO concentration of the upper water levels was relatively high; the upper oxycline was at 89–330 m, and the minimum DO concentration was 2.92 mg/L. The DO concentration remained low at 330–1111 m, and the lower oxycline formed at depths >1111 m.

There was no relationship between the isotherm of the position of M4 seamount, indicating that there is no formation of upwelling or seamount effect around the M4 seamount on a scale of 3000 m. However, there are low-value areas of DO at the bottom of the seamount, which may be due to the accumulation of organic matter and benthic organisms caused by the topography of the seamount.

The thermodynamic parameters primarily affected the upper oxycline of the OMZ. The UUO was controlled by the thermocline and pycnocline and is located below the UT and UP. The LUO was controlled by the high-salt area that is located below the LS. The thickness of the thermocline has an extremely significant negative correlation with the upper boundary of the upper oxycline, and the gradient of the thermocline has an extremely significant positive correlation with the gradient of the upper oxycline, indicating that an increase in temperature aggravates the stratification of seawater, which not only makes the oxycline shallow but also enhances the strength of the DO stratification, thereby promoting the expansion of the OMZ.

Because the DO content is high in the tropical western Pacific Ocean near the M4 seamount determining the range of the OMZ using the threshold method is challenging. The OMZ in this area is characterized as follows based on the relationship between the thermodynamic parameters, water mass, and DO: the water layer with low DO concentration between the LS and 1000 m, with considerable oxyclines between it and the upper and lower water levels. According to this definition, the OMZ at the M4 seamount is located at 266–1000 m.

CRediT authorship contribution statement

Jun Ma: Conceptualization, Formal analysis, Writing – original draft, Visualization, Funding acquisition. **Xuegang Li:** Project administration, Supervision, Funding acquisition. **Jinming Song:**

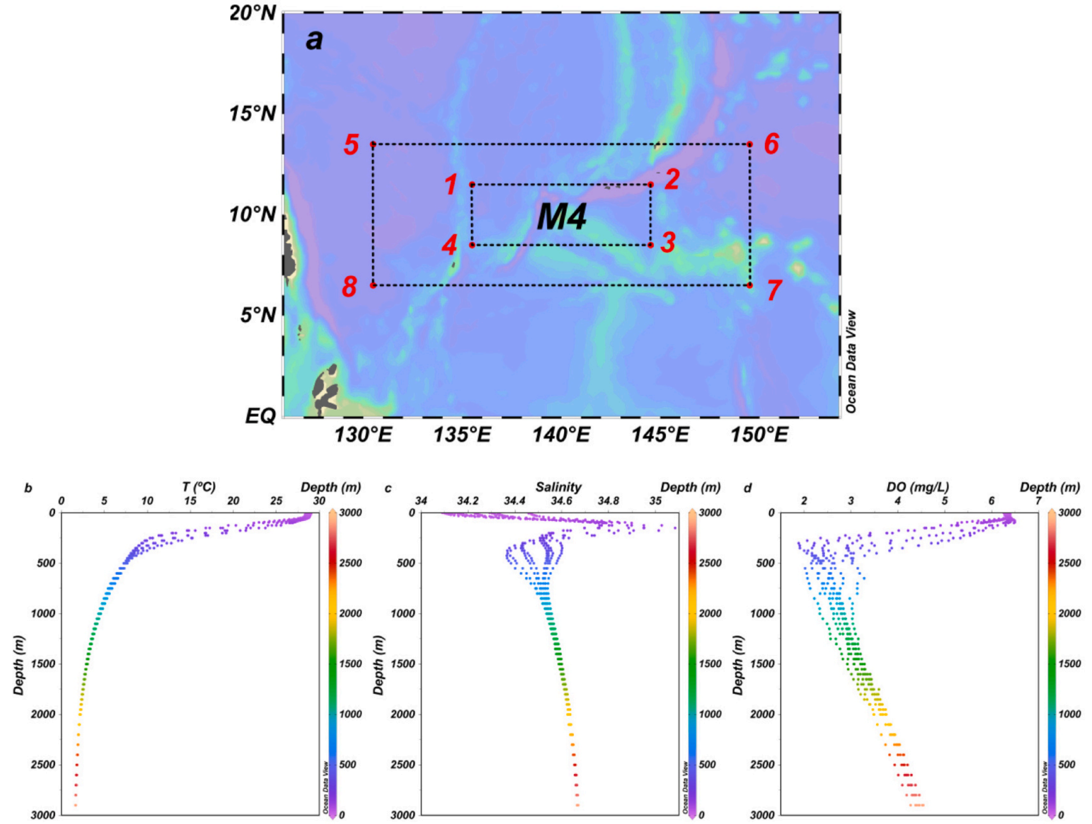

Fig. 9. Vertical distribution of T, salinity and DO in 8 stations of the Tropical Western Pacific Ocean. a) Location of 8 stations, b) Distribution of T, c) Distribution of salinity, d) Distribution of DO.

Table 2
T, salinity and DO in 8 stations of the Tropical Western Pacific Ocean.

Station	UT (m)	LT (m)	US (m)	LS (m)	UUO (m)	LUO (m)	Minimum of DO (mg/L)	Range of OMZ (m)
1	85	275	35	300	75	425	2.37	300–1000
2	95	275	35	300	95	400	2.15	300–1000
3	70	225	20	250	65	300	2.08	250–1000
4	55	225	25	225	55	300	2.39	225–1000
5	100	250	45	400	100	500	2.57	400–1000
6	125	300	45	350	120	500	2.02	350–1000
7	75	225	30	225	60	300	1.88	225–1000
8	50	225	25	250	45	300	2.90	250–1000
This study	81	203	46	266	88	330	2.92	266–1000

Methodology, Resources, Writing – review & editing, Supervision. **Lilian Wen:** Formal analysis. **Qidong Wang:** Investigation, Data curation. **Kuidong Xu:** Investigation, Funding acquisition. **Jiajia Dai:** Investigation. **Guorong Zhong:** Validation.

Declaration of Competing Interest

The authors declare that they have no known competing financial interests or personal relationships that could have appeared to influence the work reported in this paper.

Data availability

Data will be made available on request.

Acknowledgments

This study was supported by the National Natural Science Foundation of China (No. 42206135, 91958103, 41930533, 42176200, 82003787), the Shandong Provincial Natural Science Foundation (No. ZR2022QD019, ZR2020QH364), the Strategic Priority Research Program of the Chinese Academy of Sciences (No. XDB42000000, XDA19060401), the Wenhai Program of QNLM (No. 2021WHZZB0900), the National Key Research and Development Program of China (No. 2017YFA0603204), and the Marine S&T Fund of Shandong Province for the Pilot National Laboratory for Marine Science and Technology (Qingdao) (No.2022QNLM040003). We also thank the crews in "*Science*" survey vessel for their support in data collection and help in the cruise.

References

Al Azhar, M., Lachkar, Z., Levy, M., Smith, S., 2017. Oxygen minimum zone contrasts between the Arabian Sea and the bay of Bengal implied by differences in remineralization depth. Geophys. Res. Lett. 44, 11106–11114.

Ana, M., Javier, A., Carlos, V.J., Fernanda, M.M., Alicia, O., Minerva, E., Ana, M., Stuart, H., 2012. Is there a seamount effect on microbial community structure and biomass? The case study of seine and sedlo seamounts (Northeast Atlantic). PLoS ONE 7, e29526.

Bertagnolli, A.D., Stewart, F.J., 2018. Microbial niches in marine oxygen minimum zones. Nat. Rev. Microbiol. 16, 723–729.

Bridges, A.E.H., Barnes, D.K.A., Bell, J.B., Ross, R.E., Howell, K.L., 2022. Depth and latitudinal gradients of diversity in seamount benthic communities. J. Biogeogr. 49, 904–915.

Bulow, S.E., Rich, J.J., Naik, H.S., Pratihary, A.K., Ward, B.B., 2010. Denitrification exceeds anammox as a nitrogen loss pathway in the Arabian Sea oxygen minimum zone. Deep-Sea Res. I Oceanogr. Res. Pap. 57, 384–393.

Chu, P.C., Fan, C., 2019. Global Ocean synoptic thermocline gradient, isothermal-layer depth, and other upper ocean parameters. Sci. Data 6, 119.

Clark, M.R., Rowden, A.A., Schlacher, T., Williams, A., Consalvey, M., Stocks, K.I., Rogers, A.D., O'Hara, T.D., White, M., Shank, T.M., 2010. The ecology of seamounts: structure, function, and human impacts. Annu. Rev. Mar. Sci. 2, 253–278.

Dai, S., Zhao, Y., Li, X., Wang, Z., Zhu, M., Liang, J., Liu, H., Tian, Z., Sun, X., 2020. The seamount effect on phytoplankton in the tropical western Pacific. Mar. Environ. Res. 162, 105094.

D`Asaro, E., Altabet, M., Kumar, N.S., Ravichandran, M., 2020. Structure of the bay of Bengal oxygen deficient zone. Deep-Sea Res. II Top. Stud. Oceanogr. 179, 104650.

Duineveld, G., Lavaleye, M., Berghuis, E., 2004. Particle flux and food supply to a seamount cold-water coral community (Galicia Bank, NW Spain). Mar. Ecol. Prog. Ser. 277, 13–23.

Dzieciuch, M.A., 2014. Signal processing and tracking of arrivals in ocean acoustic tomography. J. Acoust. Soc. Am. 136, 2512–2522.

Engel, A., Kiko, R., Dengler, M., 2022. Organic matter supply and utilization in oxygen minimum zones. Annu. Rev. Mar. Sci. 14, 355–378.

Fawcett, S.E., Johnson, K.S., Riser, S.C., Van Oostende, N., Sigman, D.M., 2018. Low-nutrient organic matter in the Sargasso Sea thermocline: a hypothesis for its role, identity, and carbon cycle implications. Mar. Chem. 207, 108–123.

Fiedler, P.C., 2010. Comparison of objective descriptions of the thermocline. Limnol. Oceanogr. Methods 8, 313–325.

Gan, B., Wu, L., 2012. Possible origins of the western pacific warm pool decadal variability. Adv. Atmos. Sci. 29, 169–176.

Genin, A., 2004. Bio-physical coupling in the formation of zooplankton and fish aggregations over abrupt topographies. J. Mar. Syst. 50, 3–20.

Genin, A., Boehlert, G.W., 1985. Dynamics of temperature and chlorophyll structures above a seamount: an oceanic experiment. J. Mar. Res. 43, 907–924.

Hazen, E.L., Johnston, D.W., 2010. Meridional patterns in the deep scattering layers and top predator distribution in the central equatorial Pacific. Fish. Oceanogr. 19, 427–433.

Holzer, M., Primeau, F.W., 2006. The diffusive ocean conveyor. Geophys. Res. Lett. 33, L14618.

Hu, D., Wu, L., Cai, W., Gupta, A.S., Ganachaud, A., Qiu, B., Gordon, A.L., Lin, X., Chen, Z., Hu, S., 2015. Pacific western boundary currents and their roles in climate. Nature 522, 299–308.

Ito, T., Deutsch, C., 2013. Variability of the oxygen minimum zone in the tropical North Pacific during the late twentieth century. Glob. Biogeochem. Cycles 27, 1119–1128.

Johari, A., Akhir, M.F., 2019. Exploring thermocline and water masses variability in southern South China Sea from the World Ocean database (WOD). Acta Oceanol. Sin. 38, 38–47.

Karstensen, J., Stramma, L., Visbeck, M., 2008. Oxygen minimum zones in the eastern tropical Atlantic and Pacific oceans. Prog. Oceanogr. 77, 331–350.

Kawabe, M., Fujio, S., 2010. Pacific Ocean circulation based on observation. J. Oceanogr. 66, 389–403.

Keeling, R.F., Körtzinger, A., Gruber, N., 2010. Ocean deoxygenation in a warming world. Annu. Rev. Mar. Sci. 2, 199–229.

Keil, Richard, G., Biladeau, Christina, Neibauer, Jacquelyn, A., Devol, Allan, 2016. A multiproxy approach to understanding the "enhanced" flux of organic matter through the oxygen-deficient waters of the Arabian Sea. Biogeosciences 13, 2077–2092.

Lai, X., Li, X., Song, J., Ma, J., Yuan, H., Duan, L., Li, N., Yang, Z., 2022. Biogeochemical characteristics and microbial response to indicate degradation of organic matter around pair-summit seamounts in the tropical Western Pacific Ocean. Ecol. Indic. 136, 108637.

Lee, M.-A., Chao, M.-H., Weng, J.-S., Lan, Y.-C., Lu, H.-J., 2011. Diel distribution and movement of sound scattering layer in kuroshio waters, northeastern Taiwan. J. Mar. Sci. Technol. 19, 253–258.

Levin, L.A., 2018. Manifestation, drivers, and emergence of open ocean deoxygenation. Annu. Rev. Mar. Sci. 10, 229–260.

Li, G., Cheng, L., Zhu, J., Trenberth, K.E., Mann, M.E., Abraham, J.P., 2020. Increasing ocean stratification over the past half-century. Nat. Clim. Chang. 10, 1116–1123.

Li, Y., Zhan, Z., Xu, K., 2021. Paragorgia papillata sp. Nov., a new bubblegum coral (Octocorallia: Paragorgiidae) from a seamount in the tropical Western Pacific. Journal of Oceanology and Limnology 39, 1758–1766.

Ma, J., Song, J., Li, X., Yuan, H., Li, N., Duan, L., Wang, Q., 2019. Environmental characteristics in three seamount areas of the tropical Western Pacific Ocean: focusing on nutrients. Mar. Pollut. Bull. 143, 163–174.

Ma, J., Song, J., Li, X., Yuan, H., Li, N., Duan, L., Wang, Q., 2020a. Control factors of DIC in the Y3 seamount waters of the tropical Western Pacific Ocean. J.Oceanol. Limnol. 38, 1215–1224.

Ma, J., Song, J., Li, X., Yuan, H., Li, N., Duan, L., Wang, Q., 2020b. Effects of Y3 seamount on nutrients influencing the ecological environment in the tropical Western Pacific Ocean. Earth Sci. Front. 27, 322–331 (in Chinese with English abstract).

Ma, J., Song, J., Li, X., Wang, Q., Sun, X., Zhang, W., Zhong, G., 2021a. Seawater stratification vs. Plankton for oligotrophic mechanism: a case study of M4 seamount area in the tropical Western Pacific Ocean. Mar. Environ. Res. 169, 105400.

Ma, J., Song, J., Li, X., Wang, Q., Yuan, H., Li, N., Duan, L., 2021b. Analysis of differences in nutrients chemistry in seamount seawaters in the kocebu and M5 seamounts in tropical Western Pacific Ocean. J.Oceanol. Limnol. 39, 1662–1674.

Ma, J., Song, J., Li, X., Wang, Q., Zhong, G., 2021c. Multidisciplinary indicators for confirming the existence and ecological effects of a Taylor column in the tropical Western Pacific Ocean. Ecol. Indic. 127, 107777.

Ma, J., Song, J., Li, X., Wang, Q., Zhong, G., Yuan, H., Li, N., Duan, L., 2021d. The OMZ and its influence on POC in the tropical Western Pacific Ocean: based on the survey in march 2018. Front. Earth Sci. 9, 632229.

Ma, J., Li, X., Song, J., Wang, Q., Wen, L., Xu, K., Zhong, G., Dai, J., Xing, J., Tian, D., 2023. Relationship and stratification of multiple marine ecological indicators: a case study in the M2 seamount area of the Western Pacific Ocean. Ecol. Indic. 146, 109804.

Misic, C., Bavestrello, G., Bo, M., Borghini, M., Castellano, M., Covazzi Harriague, A., Massa, F., Spotorno, F., Povero, P., 2012. The "seamount effect" as revealed by organic matter dynamics around a shallow seamount in the Tyrrhenian Sea (Vercelli seamount, western Mediterranean). Deep-Sea Res. I Oceanogr. Res. Pap. 67, 1–11.

Morgan, N.B., Goode, S., Roark, E.B., Baco, A.R., 2019. Fine scale assemblage structure of benthic invertebrate megafauna on the North Pacific seamount mokumanamana. Front. Mar. Sci. 6, 715.

MouriÑO, B., FernÁNdez, E., Serret, P., Harbour, D., Sinha, B., Pingree, R., 2001. Variability and seasonality of physical and biological fields at the great meteor tablemount (subtropical NE Atlantic). Oceanol. Acta 24, 167–185.

Naqvi, S.W.A., Bange, H.W., Farias, L., Monteiro, P.M.S., Scranton, M.I., Zhang, J., 2010. Marine hypoxia/anoxia as a source of CH4 and N2O. Biogeosciences 7, 2159–2190.

Pachiadaki, M.G., Sintes, E., Bergauer, K., Brown, J.M., Record, N.R., Swan, B.K., Mathyer, M.E., Hallam, S.J., Lopez-Garcia, P., Takaki, Y., Nunoura, T., Woyke, T., Herndl, G.J., Stepanauskas, R., 2017. Major role of nitrite-oxidizing bacteria in dark ocean carbon fixation. Science 358, 1046–1050.

Paulmier, A., Ruiz-Pino, D., 2009. Oxygen minimum zones (OMZs) in the modern ocean. Prog. Oceanogr. 80, 113–128.

Pawlowicz, R., McDougall, T., Feistel, R., Tailleux, R., 2012. An historical perspective on the development of the thermodynamic equation of Seawater–2010. Ocean Sci. 8, 161–174.

Priou, P., Nikolopoulos, A., Flores, H., Gradinger, R., Kunisch, E., Katlein, C., Castellani, G., Linders, T., Berge, J., Fisher, J.A., 2021. Dense mesopelagic sound scattering layer and vertical segregation of pelagic organisms at the Arctic-Atlantic gateway during the midnight sun. Prog. Oceanogr. 196, 102611.

Resplandy, L., 2018. Climate change and oxygen in the ocean. Nature: international weekly journal of. Science 557, 314–315.

Safarov, J., Millero, F., Feistel, R., Heintz, A., Hassel, E., 2009. Thermodynamic properties of standard seawater: extensions to high temperatures and pressures. Ocean Sci. 5, 235–246.

Saito, M.A., McIlvin, M.R., Moran, D.M., Santoro, A.E., Dupont, C.L., Rafter, P.A., Saunders, J.K., Kaul, D., Lamborg, C.H., Westley, M., Valois, F., Waterbury, J.B., 2020. Abundant nitrite-oxidizing metalloenzymes in the mesopelagic zone of the tropical Pacific Ocean. Nat. Geosci. 13, 355–362.

Sánchez-Leal, R.F., Bellanco, M.J., Naranjo, C., García-Lafuente, J., González-Pola, C., 2020. On the seasonality of waters below the seasonal thermocline in the Gulf of Cádiz. Cont. Shelf Res. 204, 104190.

Schmidtko, S., Stramma, L., Visbeck, M., 2017. Decline in global oceanic oxygen content during the past five decades. Nature 542, 335–339.

Shen, C., Lu, B., Li, Z., Zhang, R., Chen, W., Xu, P., Yao, H., Chen, Z., Pang, J., Wang, C., 2021. Community structure of benthic megafauna on a seamount with cobalt-rich ferromanganese crusts in the northTropical Western Pacific Ocean. Deep-Sea Res. I Oceanogr. Res. Pap. 178, 103661.

Shenoy, D.M., Iyyappan, S., Uskaikar, H., Kurian, S., Pj, V., Shirodkar, G., Gauns, M., Naqvi, S.W.A., 2020. Variability of dissolved oxygen in the Arabian Sea oxygen minimum zone and its driving mechanisms. J. Mar. Syst. 204, 103310.

Stramma, L., Johnson, G.C., Sprintall, J., Mohrholz, V., 2008. Expanding oxygen-minimum zones in the tropical oceans. Science 320, 655–658.

Stramma, L., Visbeck, M., Brandt, P., Tanhua, T., Wallace, D., 2009. Deoxygenation in the oxygen minimum zone of the eastern tropical North Atlantic. Geophys. Res. Lett. 36, L20607.

Stramma, L., Schmidtko, S., Levin, L.A., Johnson, G.C., 2010. Ocean oxygen minima expansions and their biological impacts. Deep-Sea Res. I 57, 587–595.

Stramma, L., Prince, E.D., Schmidtko, S., Luo, J., Hoolihan, J.P., Visbeck, M., Wallace, D. W.R., Brandt, P., Körtzinger, A., 2012. Expansion of oxygen minimum zones may reduce available habitat for tropical pelagic fishes. Nat. Clim. Chang. 2, 33–37.

Wang, B., Wu, R., Lukas, R., 2000. Annual adjustment of the thermocline in the tropical Pacific Ocean. J. Clim. 13, 596–616.

Wang, F., Li, Y., Zhang, Y., Hu, D., 2013. The subsurface water in the North Pacific tropical gyre. Deep-Sea Res. I Oceanogr. Res. Pap. 75, 78–92.

Wang, Q., Song, J., Li, X., Ma, J., Yuan, H., Li, N., Duan, L., 2021. Characteristics and biogeochemical effects of oxygen minimum zones in typical seamount areas, tropical Western Pacific. J. Oceanol. Limnol. 39, 1651–1661.

Wen, L., Li, X., Song, J., Ma, J., 2022. Transparent exopolymer particle (TEP) and its impact on marine carbon transport along the East China Sea coast. Ecol. Indic. 137, 108791.

Williams, B., Grottoli, A.G., 2010. Recent shoaling of the nutricline and thermocline in the western tropical Pacific. Geophys. Res. Lett. 37, 707–716.

Wishner, K.F., Gelfman, C., Gowing, M.M., Outram, D.M., Rapien, M., Williams, R.L., 2008. Vertical zonation and distributions of calanoid copepods through the lower oxycline of the Arabian Sea oxygen minimum zone. Prog. Oceanogr. 78, 163–191.

Wishner, K.F., Outram, D.M., Seibel, B.A., Daly, K.L., Williams, R.L., 2013. Zooplankton in the eastern tropical North Pacific: boundary effects of oxygen minimum zone expansion. Deep-Sea Res. I Oceanogr. Res. Pap. 79, 122–140.

Worcester, P.F., Dzieciuch, M.A., Mercer, J.A., Andrew, R.K., Dushaw, B.D., Baggeroer, A.B., Heaney, K.D., D'Spain, G.L., Colosi, J.A., Stephen, R.A., 2013. The North Pacific acoustic laboratory deep-water acoustic propagation experiments in the Philippine Sea. J. Acoust. Soc. Am. 134, 3359–3375.

Wu, X., Hutchings, P., Murray, A., Xu, K., 2021. Laetmonice iocasica sp. Nov., a new polychaete species (Annelida: Aphroditidae) from seamounts in the tropical Western Pacific, with remarks on L. Producta grube, 1877. J.Oceanol. Limnol. 39, 1805–1816.

Xu, K., 2021. Exploring seamount ecosystems and biodiversity in the tropical Western Pacific Ocean. J.Oceanol. Limnol. 39, 1585–1590.

Xu, Y., Zhan, Z., Xu, K., 2021. Morphology and phylogeny of Chrysogorgia pinniformis sp. nov. and C. varians sp. nov., two golden corals from the Caroline seamounts in the tropical Western Pacific Ocean. J.Oceanol. Limnol. 39, 1767–1789.

Yang, S.L., Wu, Y.M., Zhang, B.B., Zhang, Y., Fan, W., Jin, S.F., Dai, Y., 2017. Relationship between fishing grounds temporal-spatial distribution of Thunnus obesus and thermocline characteristics in the Western and Central Pacific Ocean. Ying Yong Sheng Tai Xue Bao 28, 281–290.

Yesson, C., Clark, M.R., Taylor, M.L., Rogers, A.D., 2011. The global distribution of seamounts based on 30 arc seconds bathymetry data. Deep-Sea Res. I Oceanogr. Res. Pap. 58, 442–453.

Zhan, R., Wang, Y., Wen, M., 2013. The SST gradient between the southwestern Pacific and the western Pacific warm pool: a new factor controlling the northwestern Pacific tropical cyclone genesis frequency. J. Clim. 26, 2408–2415.

Zhang, Y., Wu, D., Lin, X., 2006. A study of thermocline and pycnocline calculations in the East China Sea in summer. In: Periodical of Ocean University of China, 36, pp. 1–7 (in Chinese with English abstract).